Robotica (2016) volume 34, pp. 483–496. © Cambridge University Press 2014
doi:10.1017/S0263574714001593

Uphill and level walking of a three-dimensional biped quasi-passive walking robot by torso control

Ying Cao†*, Soichiro Suzuki‡ and Yohei Hoshino‡

†*Graduate School of Engineering, Kitami Institute of Technology, Kitami, Hokkaido, Japan*
‡*Department of Mechanical Engineering, Kitami Institute of Technology, Kitami, Hokkaido, Japan*

(Accepted June 2, 2014. First published online: July 15, 2014)

SUMMARY
Passive walking robots can walk on a slight downward slope powered only by gravity. We propose a novel control strategy based on forced entrainment to stabilize a three-dimensional quasi-passive walking robot in uphill and level walking by using torso control in the frontal plane and synchronization of lateral motion with swing leg motion. We investigated the robot's walking energy efficiency, energy transformation, and transfer in simulation. The results showed that the proposed method is effective and energy-efficient for uphill and level walking. The relationship between energy utilization rate of actuation and energy efficiency of the robot was revealed, and mechanical energy transformation and transfer were characterized.

KEYWORDS: Biped robot; Passive walking; Torso control; Forced entrainment; Energy efficiency; Energy transformation; Energy transfer.

1. Introduction

A passive walking robot can walk down a gentle slope powered only by gravity without any actuator and control.[1] Its similarity to human gait and high energy efficiency implies that human walking may sufficiently utilize passive dynamics. Study of passive walking contributes to an understanding of the mechanism of biped walking and to design and control of biped robots.

Passive walking is stable under the condition of appropriate design, initial state, and slope angle.[2] However, it is difficult to stabilize passive walking robots in variable environments, such as a variable slope, and addition of some control is therefore necessary to stabilize passive walking robots. Some researchers have focused on actuation of the hip, ankle, and knee. Collins *et al*.[3] demonstrated that quasi-passive walking robots can walk on a flat ground with startling human-like gait only with simple control, such as ankle push-off or hip actuation. Harata *et al*.[4] reported a biped robot with only knee actuation controlled by a parametric excitation method. Tedrake *et al*.[5] investigated a three-dimensional (3D) biped passive walking robot "Toddler" with large curved feet and active ankle joints, rolling motions of which are controlled by utilizing a sine oscillator in order to excite the overall lateral motion of the robot. They used "Toddler" to test the utility of motor learning and demonstrated that "Toddler" could learn to walk on flat ground by using its passive walking trajectory as the target.[3] A similar quasi-passive walking robot proposed by Nakanishi *et al*.[6] also has curved feet and excites its lateral motion by a sine oscillator. The difference is that the oscillator moves from side to side on its hip axis in Nakanish *et al*.'s study.

Some researchers have focused on pitching control of the torso based on planar walking models. McGeer[7] added a torso to his planar walking model and maintained a constant gesture of the torso by using a PD controller. Wisse *et al*.[8] investigated a planar walking model with the upper body constrained to the middle angle of the two legs. Narukawa *et al*.[9] showed that a planar walking model can walk on level ground efficiently by utilizing torso and swing leg control. However, few researchers have focused on rolling control of the torso based on 3D passive walking models. In normal walking of humans, the torso not only pitches in the sagittal plane but also rolls in the frontal plane.

* Corresponding author. E-mail: d1171508033@std.kitami-it.ac.jp

https://doi.org/10.1017/S0263574714001593 Published online by Cambridge University Press

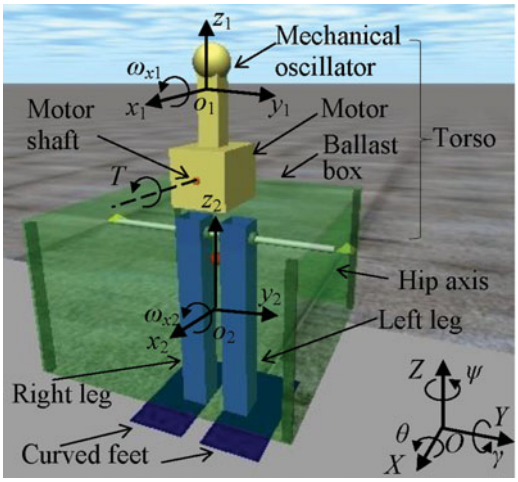


Fig. 1. Overview of simulation model of the robot.

Kuo[10] reported that torso control can be utilized to stabilize lateral motion of 3D passive walking robot, but the method was energy-inefficient to his walking model and was thus not investigated sufficiently.

In our previous study, it was experimentally demonstrated that synchronization of the period of lateral motion T_L with the period of swing leg motion T_S was a necessary condition for stable 3D passive walking.[11] In the next step, a mechanical oscillator actuated by a motor was mounted on a 3D passive walking robot with spherical feet, and can roll in the frontal plane in order to control T_L and to synchronize T_L with T_S.[12,13] The proposed method is also examined by our experimental robot.[13] This method is analogous to moving the upper body to the left or right in the frontal plane in human walking. Based on this stabilization method, turning and climbing were also realized by improving torso control.[14]

The energy efficiency of walking is often evaluated by the specific mechanical cost of transport (c_{mt}), which focuses on the mechanical energy consumption. In the walking of a biped robot, the work performed by actuators is transformed to mechanical energy of the robot. The efficiency of energy transformation can be evaluated by energy utilization rate (r_{eu}), which focuses on the mechanical energy generated by actuators. However, the relationship between r_{eu} and c_{mt} is still unclear. Besides, the mechanical energy is transferred between segments of the robot in walking and allows the legs to move forward even without actuators at the hip. However, the process in quasi-passive walking has not been investigated sufficiently.

In this study, we focus on the control, energy efficiency, energy transformation, and energy transfer of the robot in uphill walking and level walking. First, a simulation model of the robot is introduced, and the previous control method is improved to realize level and uphill walking on a variable slope. The improved control method is examined by simulations to apply it to our experimental robot in future work. Second, c_{mt} is extended to measure the energy efficiency of uphill walking. Energy transformation in walking and the relationship between r_{eu} and c_{mt} is investigated by using the robot in our current study. Finally, energy transfer and energy transformation from the torso to the legs in walking are investigated to explain why the robot can walk on a variable slope with only an actuator of the torso.

2. Simulation Model

The quasi-passive walking robot consists of two straight legs and a torso, and the torso includes a mechanical oscillator, a motor, and a ballast box, as shown in Fig. 1. The structure and the mass distribution of the simulation model is almost the same as our experimental robot, and thus the control algorithm examined by simulation can be applied to the experimental robot. The robot has three joints: two passive joints connecting the legs with a hip axis, and one active joint driven by a motor that actuates a mechanical oscillator in the frontal plane. Therefore the pitch motion of the torso is uncontrollable, but the rolling motion of the mechanical oscillator around the x_1-axis is controllable.

https://doi.org/10.1017/S0263574714001593 Published online by Cambridge University Press

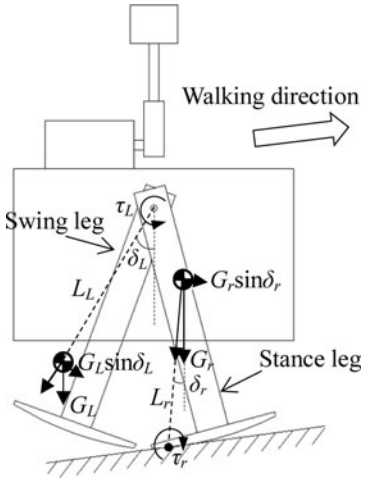


Fig. 2. Rotational torques of the legs generated by gravity in uphill walking.

The ballast box is fixed at the hip axis to mount the motor and the mechanical oscillator on the passive walking robot, and the ballast box has the function of ballast to keep the mechanical oscillator upright. The mechanical oscillator is analogous to the upper portion of the human torso above the waist. The soles of the feet of the robot are spherical. The centers of the spheres are designed to be higher than the center of mass of the robot in order to make the robot stable in a standing posture. The robot is quite robust against disturbances due to this design of the feet.

The geometric design of the feet is symmetric with respect to front and back, but the mass distribution of the feet is not. The centers of masses of the feet are regulated backward so that the swing leg can naturally swing forward even on a slight upward slope, as shown in Fig. 2. In experimental robot the mass distribution of the feet can be changed by putting a weight on each foot. The gravity of the left leg is presented by G_L, $G_L\sin\delta_L$ is the component force of G_L, L_L is the moment arm of $G_L\sin\delta_L$, and τ_L is the rotational torque of the left leg generated by $G_L\sin\delta_L$.

When the robot walks on a slight upward slope, because of the design of the spherical foot sole, a rotational torque is generated around the contact point between the stance foot and the ground, as shown in Fig. 2. The gravity of the robot is represented by G_r, $G_r\sin\delta_r$ is the component force of G_r, L_r is the moment arm of $G_r\sin\delta_r$, and τ_r is the rotational torque of the robot generated by $G_r\sin\delta_r$.

At least six generalized coordinates are necessary to describe the dynamics of the robot by Lagrangian mechanics: three coordinates are used to describe the orientation of the stance foot and the other three are used to describe the rotational angles of the three joints. In addition, the robot is a non-holonomic system because the spherical stance foot rolls on the ground in walking. In order to reduce the mathematical complexity, Open Dynamics Engine[15] (ODE; a 3D rigid-body physical simulation engine) was used to conduct simulations.

In order to describe the position and orientation of the robot in ODE simulation, the global coordinate *O–XYZ* is defined as shown in Fig. 1. The orientation of the ballast box relative to the coordinate *O–XYZ* is determined by the sequence of rolling (θ), pitching (γ), and yawing (ψ) about the axes of *O–XYZ*. The ballast box and the mechanical oscillator have the same pitch (γ) and yaw (ψ) angles but can roll independently. Therefore, the relative roll angle of the mechanical oscillator to the ballast box is defined as θ_w, as shown in Fig. 3. The ballast box and the legs have the same roll angle (θ) but different yaw and pitch angles. The pitch angles of the left and right legs are therefore denoted by γ_L and γ_R, respectively, and the yaw angles of the left and right legs are denoted by ψ_L and ψ_R, respectively. Finally, the state vector of the robot is described as

$$q = [\theta, \theta_w, \gamma, \gamma_L, \gamma_R, \psi, \psi_L, \psi_R, \dot{\theta}, \dot{\theta}_w, \dot{\gamma}, \dot{\gamma}_L, \dot{\gamma}_R, \dot{\psi}, \dot{\psi}_L, \dot{\psi}_R]\,. \tag{1}$$

The body coordinates of the mechanical oscillator and the ballast box are defined as $o_1 - x_1y_1z_1$ and $o_2 - x_2y_2z_2$, respectively, as shown in Fig. 1. The origins of the coordinates o_1 and o_2 are fixed

https://doi.org/10.1017/S0263574714001593 Published online by Cambridge University Press

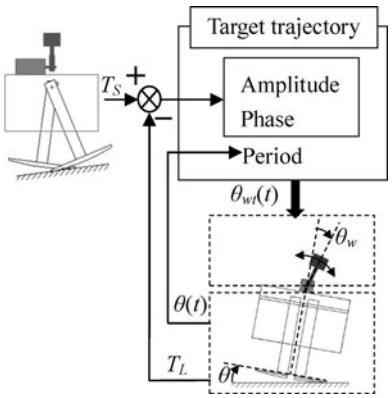


Fig. 3. Stabilization control algorithm.

on the centers of masses of the mechanical oscillator and the ballast box, respectively. The body coordinates of the legs are omitted in Fig. 1. These body coordinates are used in the calculation of rotational kinetic energy of the segments of the robot.

In the single support phase, the spherical stance foot purely rolls on the ground without slip, and the swing leg swings ahead like a pendulum. The swing leg continues to leave the ground until the roll angle θ becomes 0. The double support phase is assumed to be instantaneous, and the motion of the swing foot reaching the ground is regarded as heel-strike. The heel-strike is assumed to be inelastic and without sliding. The frictions of the joints are set to 0 in the ODE simulation.

3. Stabilization Control

3.1. Control algorithm and simulation of uphill and level walking

In variable environments, the gait of a quasi-passive walking robot will often be changed and thus may become unstable because of the disturbance of environments. If the change of gait can be utilized to stabilize the robot in an appropriate way, the environmental adaptability of the robot may be improved. Based on this idea, the periodic lateral motion of the robot in walking is utilized to entrain the periodic motion of the mechanical oscillator by utilizing a forced Van der Pol oscillator. The mechanical oscillator can excite or damp the lateral motion in order to control the period of lateral motion T_L by adjusting the phase of the mechanical oscillator.

Furthermore, in order to stabilize the robot in uphill and level walking, T_L has to be synchronized with the period of swing leg motion T_S. Swing leg motion is passive and therefore T_S cannot be controlled directly. Thus, T_L is controlled and synchronized with T_S by the motion of the mechanical oscillator in the frontal plane. The target trajectory of the mechanical oscillator θ_{wt} is planned according to the period, amplitude, and phase, as shown in Fig. 3. The motor is controlled by a simple PD controller to trace the target trajectory of the mechanical oscillator.

The period of the target trajectory is controlled on the basis of forced entrainment, which is an interesting phenomenon in nonlinear vibrations,[16] and forced entrainment is realized on the basis of forced Van der Pol equation as follows:[13]

$$\ddot{y} - \varepsilon(1 - y^2)\dot{y} + \Omega_V^2 y = K\theta, \tag{2}$$

where the roll angle θ of lateral motion of the robot is input for Eq. (2) as a periodic forcing function. The self-excited angular frequency of Eq. (2) is represented by Ω_V, and the angular frequency of θ is represented by ω. If $\Omega_V \cong \omega$ or the coefficient K is sufficiently large, system (2) indicates a phase-locking phenomenon and θ will entrain y. According to forced entrainment, the periods of y and $\dot{y}$ are synchronized to the period of θ, and the phase of $\dot{y}$ is the same as that of θ, but there is a phase difference of $\pi/2$ between y and θ. Therefore, numerical solutions of y and $\dot{y}$ are utilized to control the period of θ_{wt}, and the period of the target trajectory θ_{wt} is also synchronized with the period of lateral motion θ.

https://doi.org/10.1017/S0263574714001593 Published online by Cambridge University Press

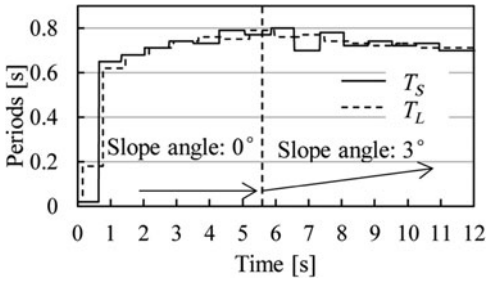


Fig. 4. Synchronization of the period of lateral motion T_L with the period of swing leg motion T_S.

The amplitude of the target trajectory β is the maximum value of θ_{wt} in one period and is controlled by a proportional integral (PI) algorithm,

$$\beta = K_P(T_S - T_L) + K_I \int_0^t (T_S - T_L)\,\mathrm{d}t, \tag{3}$$

where K_P and K_I are the proportional and integral gains, respectively. The PI algorithm can suppress steady state error to synchronize T_L with T_S. Moreover, a simple method is used to deal with integral windup, which will cause large overshoots. Since the power and maximum speed of an actual motor are limited, the maximum value of the amplitude β is limited to 18° in the ODE simulations. However, the output limitation of the amplitude will cause actuator saturation. To solve this problem, a simple method is used by setting the maximum value of output of the integral component to 18° . If the output is larger than the maximum value, the integral calculation of the integral component will be stopped.

The target trajectory θ_{wt} is determined by the periods of y and $\dot{y}$, amplitude β, and phase difference φ as follows:[13]

$$\theta_{wt} = \beta\left(\frac{1}{c_1}\dot{y}\cos\varphi - \frac{1}{c_2}y\sin\varphi\right), \tag{4}$$

where c_1 and c_2 are the amplitudes of y and $\dot{y}$. When β is positive, the phase difference φ between the target trajectory θ_{wt} and the roll angle θ is set to 90° or −90° in order to increase or decrease T_L most efficiently, respectively.[13] When φ is set to 90°, the phase difference is automatically selected as 90° or –90° according to the sign of β, because –sin90° is equal to sin(−90°) and cos(±90°) is equal to 0.

In order to generate the period of the target trajectory, the forced Van der Pol equation needs a periodical input of θ. The initial condition of the robot is thus set to $q = [0.12, 0\ldots0]$ so as to let the robot periodically roll first. In the ODE simulation, the robot walked on a path with slope angle changed from 0° to 3° and started to walk on the slope of 3° after 5.59 [s]. The changes in T_L and T_S are shown in Fig. 4. The period of lateral motion T_L was synchronized with T_S, and the robot was stabilized despite the change in slope angle. The forced entrainment of lateral motion and motion of the mechanical oscillator is characterized by the roll angle θ and θ_w, as shown in Fig. 5. In this figure, θ_w and θ_{wt} are the actual trajectory and the target trajectory of the mechanical oscillator, respectively. As shown in Fig. 5, T_L is defined as the period of θ. The pitch angles of the legs are shown in Fig. 6. A stance phase and a swing phase of the right leg are also shown in Fig. 6. The period of swing-leg motion T_S begins when the pitch angle γ_L matches γ_R, and the end of the period T_S is defined as the moment when γ_L matches γ_R after one period, as shown in Fig. 6.

Based on the control method mentioned above, the robot is robust against initial condition and disturbance, because the dynamics of the mechanical oscillator is always forcedly entrained into the dynamics of lateral motion in order to excite or damp the lateral motion. Even when the gait of our robot is changed in variable environments, the robot can still be stabilized.

In contrast, "Toddler"[5] is stabilized by direct excitation of a sine oscillator. As a result, the entrainment can occur only when the frequency of the sine oscillator is tuned to near the passive step frequency of the robot. Furthermore, the "Toddler" robot must be initialized in phase with

https://doi.org/10.1017/S0263574714001593 Published online by Cambridge University Press

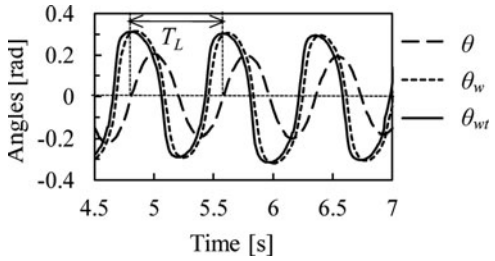


Fig. 5. Forced entrainment of the mechanical oscillator motion and lateral motion.

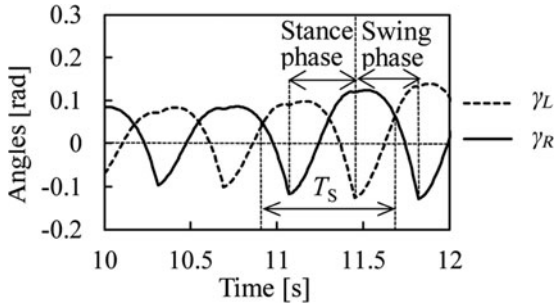


Fig. 6. Pitch angles of the legs.

the sine oscillator and the entrainment is very sensitive to disturbance in phase.[5] Consequently, the environmental adaptability of "Toddler" is worse than ours.

4. Energy Efficiency of Walking

4.1. Mechanical cost of transport in uphill and level walking

In level walking, in order to compare mechanical energy efficiencies of steady walking of different-sized robots and a human, a useful measure of energy efficiency is the specific mechanical cost of transport[3,17,18] (c_{mt}): c_{mt} = (mechanical energy used)/(weight × distance traveled), where "mechanical energy used" is divided by "weight" because different-sized robots have different weights. In quasi-passive walking, some robots only perform positive work in level walking, such as a Cornell biped,[3] and their "mechanical energy used" is thus equal to the positive work. However, for humans and most biped robots, both positive work and negative work are performed by actuators, and thus the "mechanical energy used" is equal to "$W_p - W_n$," where W_p is positive work and W_n is negative work and has negative value.

In uphill walking, a part of the mechanical work is transformed into potential energy and thus is not consumed. "Mechanical energy used" is therefore equal to "$W_p - W_n - \Delta E_p$," where ΔE_p represents the change in potential energy. Therefore, c_{mt} is extended to measure the efficiency of uphill and level walking as follows:

$$c_{mt} = \frac{W_p - W_n - \Delta E_p}{\text{weight} \times \text{distance traveled}}. \tag{5}$$

Equation (5) can still be used for passive walking robots and robots that perform only positive work. For passive walking robots, "$W_p - W_n - \Delta E_p$" is equal to "$-\Delta E_p$," which is positive in passive walking and equal to the loss of potential energy. For quasi-passive walking robots which perform only positive work in level walking, "$W_p - W_n - \Delta E_p$" is equal to W_p.

Average values of c_{mt} of our robot in level, uphill walking and passive walking are shown in Table I, which also shows c_{mt} of humans and several other biped walking robots.[19] In this table, c_{mt}

https://doi.org/10.1017/S0263574714001593 Published online by Cambridge University Press

Table I. Energy efficiencies of humans and several biped robots.

Humans and robots	c_{mt}
Humans	0.05
ASIMO	1.60
Our robot	
Uphill walking	0.108
Level walking	0.095
Passive walking	0.052
Delft's Denise	0.08
Cornell biped	0.055
McGeer's Dynamite	0.04

of uphill walking was measured when our robot walked on a 3° upward slope. In uphill walking, both "mechanical energy used" and "distance traveled" decrease in one walking cycle, and thus c_{mt} values of uphill walking and the level walking are similar. The collision at the heel strike of our robot is set to inelastic collision in the ODE simulation, and the simulation model therefore consumes more mechanical energy than some other experimental quasi-passive walking robots.

Some understanding of the energy efficiency of humans and robots can be obtained from the perspective of energy transformation. In level walking of humans, most of the mechanical energy is dissipated by humans themselves rather than by the external world. The negative work of muscles offsets most of the positive work of muscles, and little mechanical energy is dissipated at heel strike in each walking cycle. For example, during a double support phase of human walking, most of the negative work is performed by the leading leg to redirect the velocity of the center of mass and to maintain steady walking.[20] Although human walking is self-resistive, humans can walk much more efficiently than humanoid robots. Humanoid robots need to accelerate and decelerate their joints to trace a planned trajectory, and if the trajectory is planned inappropriately, much more negative work offsets its positive work. Although the walking of humanoid robots and walking of humans are both self-resistive, humans can utilize mechanical energy much more efficiently than can humanoid robots.

Energy transformation in passive and quasi-passive walking is different from that in human walking. Passive walking robots perform no work but consume potential energy in walking on a downward slope, and the loss of potential energy is dissipated at heel strike. Some quasi-passive walking robots can only perform positive work in level walking, such as a Cornell biped, and their mechanical energy is also dissipated at heel strike. Although our robot performs both positive work and negative work in walking, the robot can still walk efficiently. Moreover, passive walking robots utilize potential energy in downhill walking, but our robot performs positive work against the pull of gravity in uphill and level walking. Energy transformation of our robot should be investigated in order to understand the efficient uphill and level walking of the robot.

4.2. Energy efficiency and energy transformation

The torque of the motor is a non-conservative force (generalized force), and the mechanical energy of the robot is therefore not conserved. According to the law of conservation of energy, the relationship between mechanical work and mechanical energy of the robot is expressed as

$$W_r = \Delta E_r + E_i, \tag{6}$$

where W_r is the mechanical work performed by the motor on the robot, ΔE_r is the change in mechanical energy of the robot, and E_i is energy loss at heel strike. The work of the motor changes the mechanical energy during a single support phase, and some of the energy is dissipated at heel strike. In a single support phase without heel strike, Eq. (6) can be simplified as

$$W_r = \Delta E_r, \tag{7}$$

https://doi.org/10.1017/S0263574714001593 Published online by Cambridge University Press

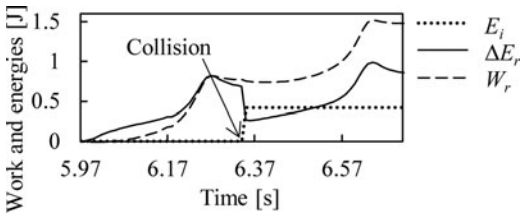


Fig. 7. Dissipated energy, change in total mechanical energy, and work performed by the motor on the robot.

which shows that the work performed by the motor only changes the mechanical energy in a single support phase.

The mechanical work and mechanical energy of the robot W_r, ΔE_r, and E_i are calculated to investigate energy transformation in walking. The mechanical oscillator and the ballast box roll in the frontal plane by actuation of the motor, as shown in Fig. 1. Therefore, work on the mechanical oscillator W_o, work on the ballast box W_b, and work on the robot W_r, which are performed by the motor only in the frontal plane, are derived by

$$W_o = \int_0^t T(t)\omega_{x1}\,\mathrm{d}t, \tag{8}$$

$$W_b = \int_0^t [-T(t)]\,\omega_{x2}\,\mathrm{d}t, \tag{9}$$

$$W_r = W_o + W_b = \int_0^t T(t)\,(\omega_{x1} - \omega_{x2})\,\mathrm{d}t, \tag{10}$$

where $T(t)$, ω_{x1}, and ω_{x2} are the torque of the motor, angular velocity of the mechanical oscillator, and angular velocity of the ballast box around the shaft of the motor, respectively. In Eq. (9), the minus sign "−" in front of $T(t)$ is due to reaction torque of the motor. In Eq. (10), $\omega_{x1} - \omega_{x2}$ is the motor speed, or the relative angular velocity of the mechanical oscillator to the ballast box.

In Eq. (6), ΔE_r is the change in mechanical energy E_r, which is the sum of potential energy, translational kinetic energy, and rotational kinetic energy of the each segment. Translational kinetic energy is calculated from the masses of the segments and the translational velocities of the centers of masses of the segments, and the rotational kinetic energy is calculated from the angular velocities of the segments and moments of inertia about their body axes through the centers of the masses. Potential energy is calculated from the height of the centers of masses from the ground.

The energy loss E_i at heel strike is expressed as

$$E_i = E_r^{t1-} - E_r^{t1+}, \tag{11}$$

where E_r^{t1-} and E_r^{t1+} are mechanical energy of the robot, "$t1-$" is the moment immediately before heel strike, and "$t1+$" is the moment immediately after heel strike.

According to Eq. (6), the work W_r, energy loss E_i, and change in mechanical energy ΔE_r in one uphill walking cycle are calculated by the ODE simulation, as shown in Fig. 7. The walking cycle begins immediately after heel strike at 5.97 s and ends immediately before heel strike at 6.71 s. The walking cycle includes a swing phase, a double support phase, and a single support phase for each leg. The results show that E_r is decreased at heel strike and energy loss E_i is increased at 6.35 s, but E_r is restored by W_r in a single support phase. The difference between W_r and $(\Delta E_r + E_i)$ can be caused by the first-order semi-implicit integrator of the ODE, in which inaccuracy in implicit integrators dampens the system energy, and inaccuracy in explicit integrators increases the system energy.[12] To minimize the error, the bounce parameter and constraint force mixing parameter (CFM) of the ODE are set to 0 and 0.0001, respectively.

https://doi.org/10.1017/S0263574714001593 Published online by Cambridge University Press

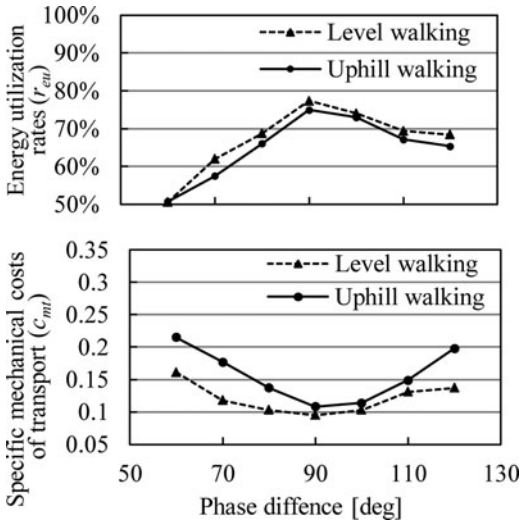


Fig. 8. Energy utilization rate and c_{mt} versus phase difference φ.

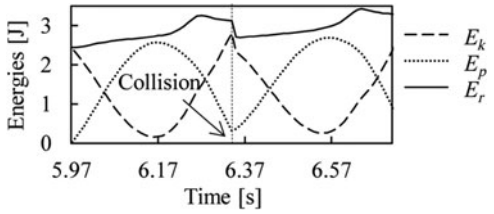


Fig. 9. Energy transformation between kinetic energy and potential energy in a walking cycle.

In order to investigate the energy utilization rate of the motor, the energy utilization rate (r_{eu}) is defined to be "$(W_p + W_n)/(W_p - W_n)$", where "$W_p + W_n$" is equal to the increase in mechanical energy of the robot inputted by the motor, and "$W_p - W_n$" is equal to the total work performed by the motor, because W_n is always negative according the definition in section 4.1. In level walking, W_p accounts for approximately 88.65% of "$W_p - W_n$" on average, and "$-W_n$" accounts for 11.35% of "$W_p - W_n$." Therefore, r_{eu} of our robot in level walking is 77.3%, which means that 77.3% of "$W_p - W_n$" is transformed into mechanical energy of the robot and the remaining 22.7% is consumed by the motor itself. More direct actuation methods can achieve higher r_{eu}, such as push-off in ankle joints of the Cornell biped,[3] and the higher r_{eu} is one reason why the Cornell biped can walk more efficiently than our robot.

In order to optimize the energy efficiency and energy utilization rate in uphill and level walking, the phase difference in the target trajectory of the mechanical oscillator is set to 90°. The relationship of phase difference φ with the energy efficiency and energy utilization rate is shown in Fig. 8. The horizontal axis is phase difference, and the vertical axis is c_{mt} and r_{eu}, respectively.

When φ is 90°, c_{mt} is 0.095 and 0.108 on average in level walking and uphill walking, respectively, and r_{eu} is 77.3% and 74.9% on average in level walking and uphill walking, respectively. When φ becomes larger or smaller than 90°, r_{eu} decreases and c_{mt} increases, because more energy is consumed by the motor itself.

The total mechanical energy of the robot E_r consists of kinetic energy E_k and potential energy E_p as shown in Fig. 9. The stance leg rolls and pitches so that the height of the center of mass of the robot changes and mechanical energy is transformed between E_p and E_k. In addition, 18.7% of E_k and 23.3% of E_k are dissipated at heel strike on average in uphill walking and level walking, respectively.

https://doi.org/10.1017/S0263574714001593 Published online by Cambridge University Press

5. Mechanical Energy Transfer and Transformation

5.1. Mechanical energy transfer from the motor to the legs

In human walking, muscles generate and dissipate mechanical energy to actuate segments, and segments of passive walking robots are actuated by gravity in passive walking. Our robot only has a motor for actuating the mechanical oscillator, and there are no actuators in other passive joints. The motor does not directly perform work on the legs, but the robot can still walk on level ground and upward slopes. This is because some of the energy is transferred to the legs during a single support phase to restore its mechanical energy by constraint forces of the joints. In order to investigate the energy transfer between the segments of the robot, the relationships between work and energy for the mechanical oscillator, ballast box, and legs in a single support phase are expressed as

$$W_o + W_{co} = \Delta E_o, \tag{12}$$

$$W_b + W_{cb} = \Delta E_b, \tag{13}$$

$$W_{cL} = \Delta E_L, \tag{14}$$

$$W_{cR} = \Delta E_R, \tag{15}$$

respectively. In Eq. (12) of the mechanical oscillator, W_o, W_{co}, and ΔE_o are the work performed by the motor on the oscillator, the work performed by constraint forces of the joint on the oscillator, and change in mechanical energy of the oscillator, respectively. The rolling motion of the mechanical oscillator is controlled by the motor, but its pitching and yawing motions are constrained by its joint, and the constraint forces perform work on the oscillator. In Eq. (13) of the ballast box, W_b, W_{cb}, and ΔE_b are the work performed by the motor on the ballast box, the work performed by the constraint forces of the joint on the ballast box, and change in mechanical energy of the ballast box, respectively. In Eq. (14) of the left leg, W_{cL} and ΔE_L are the work performed by constraint forces of the joint on the left leg and change in mechanical energy of the left leg, respectively. In Eq. (15) of the right leg, W_{cR} and ΔE_R are the work performed by the constraint forces of joint on the right leg and change in mechanical energy of the right leg, respectively. In Eqs. (12)–(15), the constraint forces of joints perform work on each segment, but the constraint forces do not change the total mechanical energy of the whole system by assuming ideal constraints. Thus,

$$W_{co} + W_{cb} + W_{cL} + W_{cR} = 0. \tag{16}$$

The work performed by the motor and mechanical energy of the robot can be directly calculated in numerical simulation, and then the work performed by constraint forces can be calculated by using Eqs. (12)–(15).

According to Eq. (12), the work performed by the motor, the constraint forces on the mechanical oscillator, and its mechanical energy in a single support phase are shown in Fig. 10(a). According to Eq. (13), the work performed by the motor, the constraint forces on the ballast box, and its mechanical energy in a single support phase are shown in Fig. 10(b). The constraint forces perform more negative work than positive work on the mechanical oscillator and ballast box (W_{co} in Fig. 10(a) and W_{ct} in Fig. 10(b)). According to Eq. (16), if W_{co} and W_{ct} are negative, W_{cL} and W_{cR} are positive. Some of the mechanical energy is transferred to the legs by the constraint forces. As shown in Fig. 10(c), W_{cL} and W_{cR} are calculated on the basis of Eqs. (14) and (15). The swing leg acquires more mechanical energy than the stance leg does in the single support phase. In the energy transfer, constraint forces neither change the total mechanical energy nor consume additional energy, and there is therefore no energy loss in the process.

5.2. Energy transformation from work of constraint forces to kinetic energy of the legs

The constraint forces of the hip joint directly increase the potential energy of the legs in rolling motion in the frontal plane. However, because the pitching motions of the legs are free, the constraint forces of the hip joint cannot directly actuate the legs to walk on a slight upward slope in the sagittal plane. In uphill walking, the forward pitching and swing motion of the legs benefit from its design, as shown in Fig. 2. The swing leg swings forward because of the rotational torque τ_L produced by the gravity

https://doi.org/10.1017/S0263574714001593 Published online by Cambridge University Press

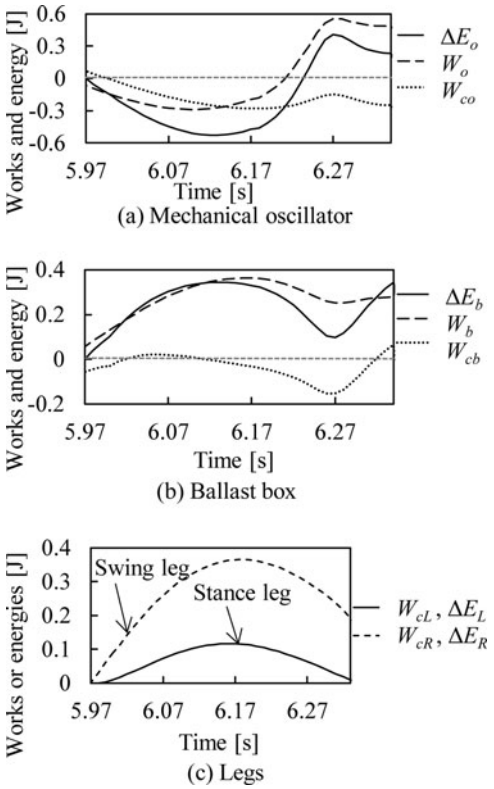


Fig. 10. Energy transfer between the segments of the robot in a single support phase.

of the swing leg about the hip axis. The stance leg rolls forward because of the inertia of the robot and the rotational torque τ_r, which is produced by the gravity of the robot around the contact point between the foot sole and the ground. In this process, the gravity of the robot performs positive work, and the potential energy of the robot is transformed to kinetic energy of pitching motion of the legs.

6. Conclusion

There are several findings or conclusions in the current study. First, we achieved uphill and level walking of a 3D quasi-passive walking robot on a variable slope in ODE simulation by torso control. The torso motion is always utilized to synchronize the lateral motion of the robot with its swing leg motion to stabilize walking. The target trajectory of the mechanical oscillator in the frontal plane is planned by controlling its phase, amplitude, and period. The proposed method will be examined by our experimental robot in future work.

Second, the energy efficiency of the robot was analyzed from the viewpoint of energy transformation. The results show that high energy utilization rate of the motor helps to increase the energy efficiency in walking. In a future work, in order to further increase energy efficiency of the robot, we will focus on improving the trajectory of the mechanical oscillator and on reducing the energy loss at heel strike by improvement in the design or by additional control. Besides, the robot can walk efficiently even though the target trajectory of the mechanical oscillator is planned. An inference from our results is that if an appropriate target trajectory can be planned, a biped robot based on a trajectory control method can also be energy-efficient.

Third, energy transfer and transformation from the torso to the legs were analyzed mathematically. The constraint forces of joints transfer mechanical energy to the legs, and potential energy is transformed to kinetic energy of the legs so that the legs can move forward.

References

1. T. McGeer, “Passive dynamic walking”, *Int. J. Robot. Res.* **9**(2), 62–82 (1990).

https://doi.org/10.1017/S0263574714001593 Published online by Cambridge University Press

2. A. Goswami, B. Espiau and A. Keramane, "Limit Cycles and Their Stability in a Passive Bipedal Gait," *Proceedings of the IEEE International Conference on Robotics and Automation,* Minneapolis, USA (Apr. 22–28, 1996) pp. 246–251.
3. S. H. Collins, A. Ruina, R. Tedrake and M. Wisse, "Efficient bipedal robots based on passive dynamic walkers," *Sci. Magazine* **307**, 1082–1085 (2005).
4. Y. Harata, F. Asano, Z. W. Luo, K. Taji and Y. Uno, "Biped gait generation based on parametric excitation by knee-joint actuation," *Robotica* **27**(7), 1063–1073 (2009).
5. R. Tedrake, T. W. Zhang, M. Fong and H. S. Seung, "Actuating a Simple 3D Passive Dynamic Walker," *Proceedings of the IEEE International Conference on Robotics and Automation*, New Orleans, LA, USA (Apr. 26–May 1, 2004) pp. 4656–4661.
6. D. Nakanishi, Y. Sueoka, Y. Sugimoto, M. Ishikawa, K. Osuka and Y. Sankai, "Emergence and Motion Analysis of 3D Quasi-Passive Dynamic Walking by Excitation of Lateral Rocking," *Proceedings of the IEEE/RSJ International Conference on Intelligent Robots and Systems*, Vilamoura (Oct. 7–12, 2012) pp. 2769–2774.
7. T. McGeer, "Dynamics and control of bipedal locomotion," *J. Theoretical Biol.* **163**(3), 277–317 (1993).
8. M. Wisse, A. L. Schwab and F. C. T. van der Helm, "Passive dynamic walking model with upper body," *Robotica* **22**(6), 681–688 (2004).
9. T. Narukawa, M. Takahashi and K. Yoshida, "Efficient walking with optimization for a planar biped walker with a torso by hip actuators and springs," *Robotica* **29**(4), 641–648 (2010).
10. A. D. Kuo, "Stabilization of lateral motion in passive dynamic walking," *Int. J. Robot. Res.* **18**(9), 917–930 (1999).
11. S. Suzuki and M. Hachiya, "Experimental study on stabilization of a three-dimensional biped passive walking robot," *J. Soc. Biomech.* (Japanese) **32**(4), 239–246 (2008).
12. M. Hachiya and S. Suzuki, "Stabilization of a biped quasi passive walking robot via periodic input", *J. Soc. Biomech.* (Japanese) **33**(1), 57–63 (2009).
13. Suzuki S, Takada M and Iwakura Y, "Stability control of a three-dimensional passive walker by periodic input based on the frequency entrainment," *J. Robot. Mechatronics* **23**(6), 1100–1107 (2011).
14. S. Suzuki, Y. Cao, M. Takada and K. Oi, "Climbing and turning control of a biped passive walking robot by periodic input based on frequency entrainment," *Adv. Eng. Forum* **2**(3), 48–52 (2011).
15. R. Smith, "Open Dynamics Engine v. 0.5 User Guide," Available at: http://ode.org; (2006).
16. R. Rand, "Lecture Notes on Nonlinear Vibrations," Available at: http://ecommons.library.cornell.edu/handle/1813/28989; (2012).
17. D. G. E. Hobbelen and M. Wisse, "Limit Cycle Walking," **In**: *Humanoid Robots, Human-like Machines* (M. Hackel, ed.), Chap. 14. (I-Tech Education and Publishing, Vienna, Austria, 2007).
18. M. Srinivasan and A. Ruina, "Computer optimization of a minimal biped model discovers walking and running," *Nature* **439**, 72–75 (2005).
19. S. H. Collins and A. Ruina, "A Bipedal Walking Robot With Efficient and Human-like Gait," *Proceedings of IEEE International Conference on Robotics and Automation,* Barcelona, Spain (Apr. 18–22, 2005) pp. 1983–1988.
20. J. M. Donelan, R. Kram and A. D. Kuo, "Simultaneous positive and negative external mechanical work in human walking," *J. Biomech.* **35**(1), 117–124 (2002).

Appendix A: Comparison of control methods

A 3D quasi-passive walking robot similar to ours is "Toddler"[5] because it has curved feet and its lateral motion is controlled by the rolling motion of ankle joints. The trajectory of ankle's rolling motion of "Toddler" is a sine function, which is determined by its amplitude and frequency. Its ankle rolling motion entrains the overall lateral motion of the robot for stable walking.

Another similar quasi-passive walking robot proposed by Nakanishi *et al*.[6] also has curved feet. The robot excites its lateral motion by an oscillator, which moves from side to side on its hip axis. The trajectory of the oscillator is also a sine function, which is determined by its amplitude and period. The actuation method is similar to "Toddler" by entraining lateral motion into a sine oscillator.

There are two major differences in the control methods between our robot and the above-mentioned two robots. First, the mechanical oscillator of our robot does not entrain the overall lateral motion, but is forcibly entrained into the lateral motion of the robot by using a forced Van der pol oscillator. As a result, the forced entrainment always occurs even when the step frequency of the robot changes in variable environments. Second, the phase of the sine oscillator is uncontrollable in the mentioned robots, but in our robot the phase of the mechanical oscillator is controllable. The motion of mechanical oscillator of our robot can excite or damp the lateral motion of the robot to control T_L, by adjusting the phase difference between the motion of the mechanical oscillator and the lateral motion of the robot. This is why our robot is very robust against disturbance in phase.

https://doi.org/10.1017/S0263574714001593 Published online by Cambridge University Press

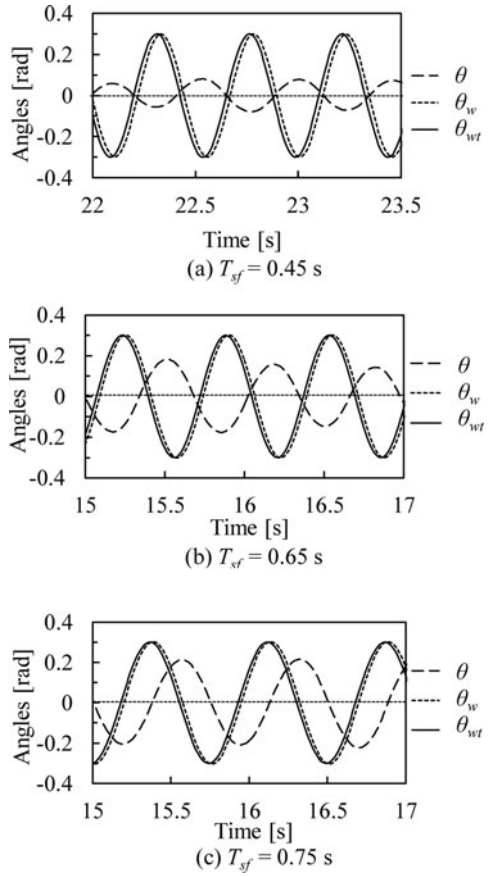


Fig. 11. Entrainment of mechanical oscillator motion and lateral motion under the excitation of a sine oscillator.

In order to compare the control methods of our robot and the above-mentioned two robots, the control method with the sine oscillator,[6] $\mathrm{d}(t) = A\sin(2\pi t / T_{sf})$, is applied to our robot in level walking. In stable walking with our control method, the amplitude of mechanical oscillator is near 0.3 rad, as shown in Fig. 5. Therefore, the amplitude of the sine function A is set to 0.3 rad to compare the results in the similar condition. When the period of the sine oscillator T_{sf} is changed from 0.4 s to 0.75 s the robot can walk stably. A longer or shorter period will cause unstable gait. The lateral motion of the robot and the mechanical oscillator motion in stable level walking are shown in Fig. 11. θ, θ_w, and θ_{wt} are the roll angle of the robot, the actual trajectory, and target trajectory of the mechanical oscillator, respectively. The period of the sine oscillator T_{sf} is set to 0.45 s, 0.65 s, and 0.75 s in Figs. 11(a)–(c), respectively. Under the control with the sine oscillator, the phase difference between θ and θ_w changes as the period T_{sf} changes. Only when T_{sf} is near 0.75 s, the phase difference is near $\pi/2$, as shown in Fig. 11(c). However, in our control method in level walking the phase difference between θ and θ_w is always constant at $\pi/2$ to excite the lateral motion of the robot, as shown in Fig. 5.

Under the control of the sine oscillator, the robot becomes sensitive to initial conditions, including initial period and phase of lateral motion of the robot. Therefore, the environmental adaptability of the method is worse than that of our method in the model of our robot.

Appendix B: Comparison of c_{mt} and r_{eu} in different control methods

The sine oscillator mentioned in Appendix A is applied to our robot. The relationship of walking period T_{sf} with c_{mt} and r_{eu} in stable level walking is shown in Fig. 12. The horizontal axis is walking period while the vertical axes are c_{mt} and r_{eu}, respectively. When T_{sf} is between 0.55 s and 0.75 s, r_{eu} is larger than 95% and c_{mt} is between 0.06 and 0.07. The maximum of r_{eu} is 97.8%, and the minimum of c_{mt} is 0.061.

https://doi.org/10.1017/S0263574714001593 Published online by Cambridge University Press

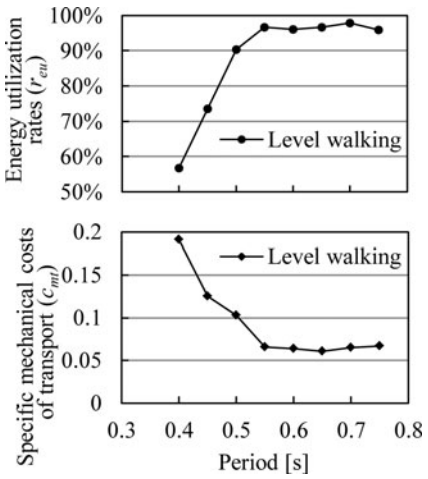


Fig. 12. Energy utilization rate and c_{mt} versus the period T_{sf}.

In comparison with our control method, the control method with sine oscillator is more energy efficient. One reason is that θ_w generated by using forced Van der Pol oscillator is not harmonic function as the sine oscillator. By comparing Fig. 5 with Fig. 11(c), it is easily seen that the amplitude, period and phase of θ and θ_w are almost the same. However, the level walking shown in Fig. 5 is less energy efficient because non-harmonic oscillation may cause deterioration of energy efficiency in the model of our robot.

https://doi.org/10.1017/S0263574714001593 Published online by Cambridge University Press